SECURITY INFORMATION

[redacted]

RM L51I23

NACA RM L51I23

UNCLASSIFIED

NACA

RESEARCH MEMORANDUM

METHOD OF ESTIMATING THE STICK-FIXED LONGITUDINAL STABILITY OF WING-FUSELAGE CONFIGURATIONS HAVING UNSWEPT OR SWEPT WINGS

By Milton D. McLaughlin

Langley Aeronautical Laboratory
Langley Field, Va.

FOR REFERENCE

NOT TO BE TAKEN FROM THIS ROOM

CLASSIFICATION CANCELLED

Authority J. W. Crowley Date 12/11/53
E O 10501
By MHA 1/8/54 See NACA
R7 1829

CLASSIFIED DOCUMENT

This material contains information affecting the National Defense of the United States within the meaning of the espionage laws, Title 18, U.S.C., Secs. 793 and 794, the transmission or revelation of which in any manner to unauthorized person is prohibited by law.

NATIONAL ADVISORY COMMITTEE
FOR AERONAUTICS

WASHINGTON

January 22, 1952

[redacted]

NACA LIBRARY
LANGLEY AERONAUTICAL LABORATORY
Langley Field, Va.

NASA Technical Library
3 1176 01436 8923

UNCLASSIFIED

NATIONAL ADVISORY COMMITTEE FOR AERONAUTICS

RESEARCH MEMORANDUM

METHOD OF ESTIMATING THE STICK-FIXED LONGITUDINAL STABILITY OF WING-FUSELAGE CONFIGURATIONS HAVING UNSWEPT OR SWEPT WINGS

By Milton D. McLaughlin

SUMMARY

A method is given for calculating the stick-fixed longitudinal stability of a wing-fuselage configuration at subcritical Mach numbers. The method applies to unswept- and swept-wing configurations. No effort has been made to include the effect of the horizontal tail but this effect could easily be calculated if the downwash values were known. In the development of the method experimental results were necessary to obtain the normal loading on the part of the fuselage in the vicinity of the wing-fuselage juncture. Experimental curves are presented which are used to predict the loading on this portion of the fuselage for other configurations.

The geometrical characteristics and the calculated contributions to lift and pitching moment of the principal parts of the wing-fuselage configurations for 23 configurations are presented. A comparison of the neutral points predicted by the method with the neutral points obtained from experiment for the 23 wing-fuselage configurations is also presented.

INTRODUCTION

Methods for computing the stick-fixed longitudinal stability of airplanes having small sweep angles (below 20°) and high aspect ratios have been developed to a point where a good degree of accuracy may be obtained with their use. In methods such as that given in reference 1 the agreement between the calculated and measured neutral points has generally been ±1.5 percent of the mean aerodynamic chord or within the accuracy with which neutral points have been evaluated from flight data. These methods do not apply, however, to configurations having large sweep angles.

[redacted]

UNCLASSIFIED

The purpose of the present paper is to derive a method which permits calculation to within a satisfactory degree of the stick-fixed static longitudinal stability of configurations having either unswept wings or wings with large sweep angles. This method applies to a wing-fuselage configuration. No effort is made to include the effect of the horizontal tail but this effect could easily be calculated if the downwash values were known. Since no generalized charts exist for estimating downwash behind swept wings, the downwash values used in the method are best obtained from experimental values on a similar wing-fuselage configuration. Theoretical procedures are used where possible to develop this method for calculating the aerodynamic forces and moments; empirical methods based on experimental results are used for those parts of the configuration for which no theory is available.

The stick-fixed neutral points of 23 wing-fuselage configurations have been calculated by the present method and a comparison with experiment is presented. The 23 wing-fuselage configurations together with pertinent information are presented in table I. Results of tests of the first 10 configurations provided experimental data which were used to obtain the variation of the normal loading on the fuselage in the vicinity of the wing-fuselage juncture. These experimental curves are used to predict the loading for similar configurations. A sample calculation of the neutral point of a wing-fuselage configuration is included in an appendix.

SYMBOLS

b	wing span perpendicular to plane of symmetry, feet
c	wing chord parallel to plane of symmetry, feet
$\bar{c}$	mean aerodynamic chord, feet
c_{av}	average wing chord $\left(S_W/b\right)$, feet
x	longitudinal coordinate measured from quarter chord of mean aerodynamic chord, feet
x_D	longitudinal distance measured from quarter chord of mean aerodynamic chord to duct inlet, feet (positive forward)
x_f	longitudinal distance measured from quarter chord of mean aerodynamic chord to a given fuselage station, feet (positive forward)
$x_{f'}$	longitudinal distance measured from fuselage nose to a given fuselage station, feet

[redacted]

x_i	longitudinal distance measured from quarter chord of mean aerodynamic chord to leading edge of intersection chord, feet (positive forward)
x_I	longitudinal distance measured from quarter chord of mean aerodynamic chord to center of pressure of carry-through section (positive forward)
y	lateral coordinate measured from plane of symmetry, feet
y_o	lateral distance to aerodynamic center of external wing measured from plane of symmetry, feet
Y	average fuselage width at wing root, feet
Y_f	finite fuselage width, feet
S	area, square feet
η	dimensionless lateral coordinate $\left(\frac{y}{b/2}\right)$
η_{cp}	spanwise center-of-pressure location on wing, fraction of semispan $\left(\frac{y_{cp}}{b/2}\right)$
A	aspect ratio $\left(b^2/S_W\right)$
λ	taper ratio $\left(\frac{\text{Tip chord}}{\text{Root chord}}\right)$
Λ	sweep angle, degrees
M	Mach number
V	velocity, feet per second
V_D	average air velocity at minimum cross section of duct inlet, feet per second
q	free-stream dynamic pressure, pounds per square foot
α	angle of attack, degrees
ϵ	downwash angle, degrees
β	angle of local air flow relative to x-axis, degrees

κ	factor used in determining $d\beta/d\alpha$
c_l	local lift coefficient $\left(\frac{\text{Local lift}}{qc}\right)$
c_{l_a}	local lift coefficient due to additional lift on wing
c_n	local normal-force coefficient $\left(\frac{\text{Local normal force}}{qc}\right)$
C_L	lift coefficient $\left(\frac{\text{Lift}}{qS_W}\right)$
C_m	pitching-moment coefficient $\left(\frac{\text{Pitching moment}}{qS_W\bar{c}}\right)$
c_{l_α}	variation of local lift coefficient with angle of attack, per degree $\left(dc_l/d\alpha\right)$
C_{L_α}	variation of lift coefficient with angle of attack, per degree $\left(dC_L/d\alpha\right)$
C_{m_α}	variation of pitching-moment coefficient with angle of attack, per degree $\left(dC_m/d\alpha\right)$
$C_{L_{\alpha_\sigma}}$	variation of center-section (fig. 1) lift coefficient with angle of attack, per degree (based on wing center-section area S_σ)
$C_{L'_{\alpha_o}}$	variation of external-wing (fig. 1) lift coefficient with angle of attack, per degree (based on external-wing area S_o)
$C_{L_{\alpha_o}}$	variation of external-wing (fig. 1) lift coefficient with angle of attack, per degree (based on total wing area S_W)
$C_{L'_{\alpha_I}}$	variation of carry-through-section (fig. 1) lift coefficient with angle of attack, per degree (based on wing carry-through area Yc_1)
$C_{L_{\alpha_I}}$	variation of carry-through-section (fig. 1) lift coefficient with angle of attack, per degree (based on total wing area S_W)

Subscripts:

o	external wing

[redacted]

W	total wing (including center section)
WF	complete configuration
σ	center section of total wing (fig. 1)
i	wing-fuselage intersection
I	wing carry-through section (fig. 1)
F	fuselage (fore and aft)
f	finite fuselage section
MAC	mean aerodynamic chord
D	intake duct
LE	leading edge of wing
ac	aerodynamic center
c/4	quarter chord
TE	trailing edge of wing
l	fuselage length
max	maximum
cp	center of pressure
av	average
exp	experimental

METHOD OF ANALYSIS

The stick-fixed neutral point of a wing-fuselage configuration is defined as the center-of-gravity location for which the slope of the curve of airplane pitching-moment coefficient against lift coefficient dC_m/dC_L is zero. In order to estimate the neutral point of a configuration it is necessary to determine the additional loading and pitching moment of the configuration. In order to determine these quantities the configuration is separated into its principal parts and the additional loading of these parts is calculated. The resultant forces and pitching moments contributed by each part are presented in coefficient form as values of C_{L_α} and C_{m_α}, respectively. From the summation of these coefficients the distance of the neutral point of the wing-fuselage configuration from the reference axis, expressed as a fraction of the mean aerodynamic chord of the wing may be found as the value of $\left(\frac{dC_m}{dC_L}\right)_{WF}$ where

$$\left(\frac{dC_m}{dC_L}\right)_{WF} = \frac{\sum \left(C_{m_\alpha}\right)_{WF}}{\sum \left(C_{L_\alpha}\right)_{WF}}$$

In the present method, the configuration is separated into the following three parts: the external wing, the fuselage fore and aft of the wing-fuselage juncture, and the wing carry-through section. (See fig. 1.) Hereinafter, the part of the fuselage fore and aft of the wing-fuselage juncture is referred to as the "fuselage." The carry-through section is considered rectangular in shape; its length is equal to the length of the wing-fuselage intersection chord and its width is the average width of the carry-through section. It is important to note, however, that whenever the total wing area is considered in the method the center-section area is the area indicated by the dotted lines in figure 1. The lift and moment coefficients for the principal parts are calculated in terms of the total wing area. The moment reference point is taken as the quarter-chord point of the mean aerodynamic chord of the total wing.

The present approach to the analysis of longitudinal stability differs somewhat from the approach presented in reference 1. In reference 1 the lift of the wing-fuselage combination is taken as the lift of an isolated wing of corresponding dimensions. Fuselage lift, therefore, must be taken as equal to the lift on the section of an isolated wing which is covered by the fuselage. Fuselage moment is obtained from an integration of the moments contributed by sections along the axis of the fuselage (equation (3.7), reference 2). The loads on each section are computed on the assumption that the flow is two-dimensional in planes perpendicular to the fuselage axis. This assumption is less accurate in the neighborhood of the wing and does not allow calculation of the loads on the wing carry-through section. For airplanes with unswept wings, however, conditions on the fuselage near the wing do not greatly influence the pitching moment of the fuselage about the neutral point of the airplane and, as a result, the method is adequate for such cases.

For swept-wing configurations the loading on the fuselage and wing carry-through section is much the same as for unswept configurations.

The wing carry-through section for swept wings, however, is located farther from the neutral point of the configuration and the longer moment arm results in a large pitching-moment contribution. The lift contribution of the wing carry-through section, therefore, must be determined as accurately as possible in order to determine satisfactorily the pitching-moment contribution. Thus the assumption that the fuselage lift can be taken as equal to the lift of the center section of an isolated wing no longer applies and the lift and moment contributions of both the fuselage and the wing carry-through sections must be obtained. In general, the method used herein is to estimate the load distribution on the fuselage and the load on the external wing by theoretical methods, whereas for the carry-through section, it is necessary to develop curves based on available experimental data for predicting the loading and the aerodynamic center. The theoretical values which were used in calculating the wing stability parameters were obtained from reference 3. Reference 3 was used because it presented a readily available uniform source of information and showed fairly good agreement when checked with experiment. The method to be used in obtaining the wing stability parameters, however, is at the discretion of the designer.

Although the method is derived for incompressible flow, it may be applied for any case of subcritical Mach number by use of the generalized Prandtl-Glauert law described in reference 4. The effects of Mach number on the neutral-point location at subcritical Mach numbers are generally small. This method is intended to apply at low lift coefficients where the drag effects are least and where the slopes of the lift curve and pitching-moment curve are linear.

CALCULATION OF STABILITY

The method of obtaining the values of $C_{L_{\alpha}}$ and $C_{m_{\alpha}}$ of the individual parts, as well as of the complete configuration, is now presented. A step-by-step procedure is utilized to facilitate the computations and the sample calculations to illustrate the method are given in the appendix.

External Wing

Calculation of $C_{L_{\alpha_O}}$.- The contribution of the external wing to the lift-curve slope $C_{L_{\alpha_O}}$ may be obtained in the following manner:

(1) Obtain the value of $C_{L_{\alpha_W}}$ for the total wing from reference 3, figure 4.

(2) Calculate the quantity $C_{L_{\alpha_W}}S_W$. (The value of β/κ of reference 3 as used in the present paper is considered to be unity.)

(3) Obtain from reference 3, figure 3, the spanwise values of $c_{l_a}c/C_Lc_{av}$ for the center section of the total wing. Each value of $c_{l_a}c/C_Lc_{av}$ is equal to the value $c_{l_\alpha}c/C_{L_{\alpha_W}}c_{av}$.

(4) Multiply each quantity $c_{l_\alpha}c/C_{L_{\alpha_W}}c_{av}$ by the product of the mean geometric chord c_{av} and the lift-curve slope for the total wing $C_{L_{\alpha_W}}$ to obtain the quantity $c_{l_\alpha}c$.

(5) Plot the values of $c_{l_\alpha}c$ against their spanwise location for the center section of the wing.

(6) Integrate the value $c_{l_\alpha}c$ spanwise over the wing center section. The integral is equal to the quantity $C_{L_{\alpha_\sigma}}S_\sigma$.

(7) Obtain the quantity $C_{L'_{\alpha_o}}S_o$ for the external wing by the formula

$$C_{L'_{\alpha_o}}S_o = C_{L_{\alpha_W}}S_W - C_{L_{\alpha_\sigma}}S_\sigma$$

(8) Obtain the lift-curve slope of the external wing based on total wing area by the relation

$$C_{L_{\alpha_o}} = \frac{C_{L'_{\alpha_o}}S_o}{S_W}$$

Calculation of $C_{m_{\alpha_o}}$.- The contribution of the external wing to pitching-moment-curve slope $C_{m_{\alpha_o}}$ is calculated as follows:

(1) Obtain from reference 3, figure 5, the spanwise center of pressure of the lift of the total wing η_{cp} as a fraction of the semispan.

[redacted]

[redacted]

(2) Perform the spanwise integration indicated in the function $\dfrac{\int_0^{Y/2} c_{l_\alpha} cy\, dy}{\int_0^{Y/2} c_{l_\alpha} c\, dy}$ over the semispan of the wing center section to obtain the spanwise center of pressure of the wing center section. In most cases the values of $c_{l_\alpha} c$ are nearly constant over the wing center section and the center of pressure is located at one-half the center-section semispan, that is $y_{\sigma_{cp}} = \frac{1}{2}\frac{Y}{2}$.

(3) Obtain the spanwise center of pressure of the external wing $y_{o_{cp}}$ from the relation

$$y_{o_{cp}} = \frac{C_{L_{\alpha_W}} S_W y_{W_{cp}} - C_{L_{\alpha_\sigma}} S_\sigma y_{\sigma_{cp}}}{C_{L_{\alpha_W}} S_W - C_{L_{\alpha_\sigma}} S_\sigma}$$

This relation is the spanwise center of pressure of the total wing corrected for the removal of the lift on the center section.

(4) Obtain the contribution of the external wing to the pitching-moment slope $C_{m_{\alpha_o}}$ by the relation

$$C_{m_{\alpha_o}} = \frac{y_{MAC} - y_{o_{cp}}}{\bar{c}} \tan \Lambda_{c/4} C_{L_{\alpha_o}}$$

If the aerodynamic center of the external wing does not lie on the quarter chord (as might be the case if other than the lifting-line theory of reference 3 were used), the distance between the quarter-chord line and the aerodynamic center must be considered in the preceding relation. The pitching-moment contribution of the external wing is then obtained by the relation

$$C_{m_{\alpha_o}} = \left(\frac{y_{MAC} - y_{o_{cp}}}{\bar{c}} \tan \Lambda_{c/4} + \frac{x_{c/4} - x_{ac}}{\bar{c}}\right) C_{L_{\alpha_o}}$$

[redacted]

Fuselage (Fore and Aft of the Intersection Chords)

Calculation of $C_{L_{\alpha_F}}$.- The contribution of the fuselage to lift-curve slope $C_{L_{\alpha_F}}$ is determined as follows:

(1) Obtain the contribution to lift-curve slope of the fore and aft fuselage sections by a graphical integration of the following formula which was derived from formula (3.3), reference 2:

$$C_{L_{\alpha_F}} = \frac{1}{57.3S_W}\left[\int_0^{LE} \frac{d\left(\frac{\pi}{2} Y_f^2 \frac{d\beta}{d\alpha}\right)}{dx_{f'}} dx_{f'} + \int_{TE}^{l} \frac{d\left(\frac{\pi}{2} Y_f^2 \frac{d\beta}{d\alpha}\right)}{dx_{f'}} dx_{f'}\right]$$

where Y_f is the width of fuselage at any station. The fuselage plan form is divided into a finite number of sections as shown by figure 1. For each of these sections the parameter $\frac{\pi}{2} Y_f^2 \frac{d\beta}{d\alpha}$ is calculated and plotted against its fuselage longitudinal station $x_{f'}$. The measured slope $\frac{d\left(\frac{\pi}{2} Y_f^2 \frac{d\beta}{d\alpha}\right)}{dx_{f'}}$ at each of these stations is proportional to the slope of the sectional lift coefficient $c_{l_{\alpha_f}}$ (per radian) of that station.

For the fuselage stations ahead of the wing values of $d\beta/d\alpha$ are obtained from figure 2 and from the following formula:

$$\frac{d\beta}{d\alpha} = 1 + \kappa \frac{C_{L_{\alpha_W}}}{A} 57.3$$

which is the variation in local air flow with angle of attack for the fuselage alone plus the additional variation caused by the presence of the wing. Figure 2 was derived from theoretical data obtained from reference 5. The parameter κ is noted to be expressed as a function of the distance forward of the intersection quarter chord $c_i/4$ which should not be confused with the quarter chord of the mean aerodynamic chord $\bar{c}/4$. For the fuselage sections behind the wing, values of $d\beta/d\alpha$ are obtained from the variation of downwash with angle of attack $d\epsilon/d\alpha$ by the formula

$$\frac{d\beta}{d\alpha} = 1 - \frac{d\epsilon}{d\alpha}$$

As no generalized charts exist for estimating downwash behind swept wings, experimental values of $d\epsilon/d\alpha$ at the location of the tail should be used when possible. The values of $d\epsilon/d\alpha$ are assumed to vary linearly from zero at the wing trailing edge to the determined value at the aft end of the fuselage. The exact value of downwash at the aft end of the fuselage is of little importance in determining fuselage lift or moments inasmuch as the lift and moment contributions of the rear section of the fuselage are very small.

Calculation of $C_{m_{\alpha_F}}$.- The contribution of the fuselage to pitching-moment-curve slope $C_{m_{\alpha_F}}$ includes the following steps:

(1) Obtain the contribution of the fore and aft fuselage sections to pitching-moment-curve slope by a graphical integration of the following formula which was derived from formula (3.7), reference 2:

$$C_{m_{\alpha_F}} = \frac{1}{57.3 S_W \bar{c}} \left[\int_0^{LE} \frac{d\left(\frac{\pi}{2} Y_f^2 \frac{d\beta}{d\alpha}\right)}{dx_{f'}} x_f \, dx_{f'} + \int_{TE}^{l} \frac{d\left(\frac{\pi}{2} Y_f^2 \frac{d\beta}{d\alpha}\right)}{dx_{f'}} x_f \, dx_{f'} \right]$$

where x_f is the longitudinal distance measured from the quarter chord of the mean aerodynamic chord to a finite fuselage station and $x_{f'}$ is the longitudinal distance measured from the fuselage nose to a finite fuselage section.

(2) Obtain, when appropriate, the additional contribution to pitching-moment-curve slope of a fuselage air-intake duct from the following formula:

$$C_{m_{\alpha_D}} = \frac{1}{57.3} \frac{V_D}{V} \frac{2 S_D x_D}{S_W \bar{c}}$$

The effect on pitching moment of the change in momentum of the air entering the intake duct obtained from this formula is illustrated in figure 3. The formula was derived from a similar unpublished formula.

Wing Carry-Through Section

Calculation of $C_{L_{\alpha_I}}$.- The contribution to lift-curve slope of the wing carry-through section $C_{L_{\alpha_I}}$ is calculated as follows:

[redacted]

(1) Obtain the contribution to lift-curve slope of the wing carry-through section from figure 4(a) by using the effective aspect ratio of the carry-through section. The lift-curve slope of the carry-through section is based on that area (intersection chord c_i times average fuselage width at wing root Y) and is presented in terms of the section-lift-curve slope of the wing at the intersection chord as $C_{L'_{\alpha_I}}/c_{l_{\alpha_i}}$. The value $c_{l_{\alpha_i}}$ may be obtained from step (5) of the outline of the contribution of the external wing to lift-curve slope $C_{L_{\alpha_O}}$.

(2) Calculate the contribution to lift-curve slope of the wing carry-through section by the relation

$$C_{L_{\alpha_I}} = \frac{C_{L'_{\alpha_I}}}{c_{l_{\alpha_i}}} c_{l_{\alpha_i}} \frac{S_I}{S_W}$$

Calculation of $C_{m_{\alpha_I}}$.- The contribution to pitching-moment-curve slope of the wing carry-through section $C_{m_{\alpha_I}}$ is obtained as follows:

(1) Obtain the aerodynamic center of the carry-through section from figure 4(b), which is a plot of the aerodynamic center of the carry-through section against sweep angle of the quarter-chord line of the wing. The aerodynamic-center location is expressed in intersection chords as the longitudinal distance from the leading edge of the intersection chord $\left(\frac{x_i}{c_i}\right)_{LE} - \left(\frac{x_I}{c_i}\right)_{ac}$.

(2) Calculate the moment arm of the aerodynamic center of the carry-through section about the reference point by the relation

$$\left(\frac{x_I}{c_i}\right)_{ac} = \left(\frac{x_i}{c_i}\right)_{LE} - \left[\left(\frac{x_i}{c_i}\right)_{LE} - \left(\frac{x_I}{c_i}\right)_{ac}\right]$$

(3) Calculate the contribution to pitching moment of the carry-through section by the relation

$$C_{m_{\alpha_I}} = \left(\frac{x_I}{c_i}\right)_{ac} \frac{c_i}{\bar{c}} C_{L_{\alpha_I}}$$

Complete Configuration

Calculation of $C_{L_{\alpha_{WF}}}$.- Obtain $C_{L_{\alpha_{WF}}}$ as a sum of the lift-curve slopes of the principal parts

$$C_{L_{\alpha_{WF}}} = C_{L_{\alpha_O}} + C_{L_{\alpha_F}} + C_{L_{\alpha_I}}$$

Calculation of $C_{m_{\alpha_{WF}}}$.- Determine $C_{m_{\alpha_{WF}}}$ by summing up the pitching-moment-curve slopes of the principal parts

$$C_{m_{\alpha_{WF}}} = C_{m_{\alpha_O}} + C_{m_{\alpha_F}} + C_{m_{\alpha_I}}$$

Calculation of neutral-point location.- Obtain the neutral-point location with respect to the reference axis, expressed as a fraction of the mean aerodynamic chord of the wing by the relation

$$\frac{C_{m_{\alpha_{WF}}}}{C_{L_{\alpha_{WF}}}} = \frac{x_{WF}}{\bar{c}}$$

DISCUSSION OF METHOD

The values of wing lift-curve slope for the total wing were obtained from reference 3 and are based on the lifting-line method of calculation. Values of wing lift-curve slope were also calculated by the method of reference 6 which is essentially a correction of unswept-wing data for sweep effects. This method has the advantage of allowing the use of values of lift-curve slope for unswept wings based on lifting-surface theory. Of the two methods the lift-curve-slope values from reference 3 showed the best over-all agreement with the experimental values for the particular configurations checked in this analysis.

In order to determine the lift-curve slope of the external wing the sectional lift is assumed to be the same as the sectional lift for a corresponding section on an isolated wing. Upflow around the body might be expected to increase the lift on the sections near the wing root. Experimental investigations of this effect are rather scarce, however, the data of reference 7 indicate that, if this expected increase does occur, it is very small. Also, flight measurements of the spanwise center of load of a wing in combination with a body have shown good agreement with the values predicted on the assumption that the sectional loading external to the body is the same as that on an isolated wing. The lift-curve slope of the external wing therefore, is assumed to be equal to the integration of the spanwise loading on the external wing in terms of the total wing area $C_{L'_{\alpha_o}} \frac{S_o}{S_W}$. The aerodynamic-center location for the external wing is then the aerodynamic-center location of the total wing corrected for the removal of the center section.

The present method for determining the values of C_{L_α} and C_{m_α} of the fuselage is based on Multhopp's method in reference 2. Good agreement is found to exist between Multhopp's method and experiment on the fore and aft sections of the fuselage as is shown in figure 5. The experimental fuselage sectional loading (fig. 5) was obtained from unpublished pressure-distribution measurements on a wing-fuselage configuration (configuration 10 in table I). For the fuselage section adjacent to the wing large disagreement can be seen between theory and experiment. The large difference in loading on the sections immediate to the wing was caused by the wing and in the present method this difference in loading is considered to be part of the wing carry-through loading.

Multhopp's method does not apply for the wing carry-through section. An effort was made, therefore, to obtain from experiment the loading of the carry-through section and its possible variations with the wings of various sweep angles and aspect ratios. These experimental curves could then be used to predict the loading on similar carry-through sections for other configurations. A limited amount of experimental pressure-distribution data was available on loadings of the carry-through section; however, a larger amount of data was available on the over-all characteristics of wing-fuselage configurations. From the wing-fuselage data and the isolated-wing data the experimental values for the wing-fuselage and total wing were obtained. By using the present method, the contribution to stability of the fore and aft fuselage sections was calculated and the effect of the wing center section was calculated and subtracted from the experimentally measured contribution of the total wing. The contributions to stability of the wing carry-through section were then found as

$$C_{L_{\alpha_I}} = \left(C_{L_{\alpha_{WF}}}\right)_{exp} - \left[\left(C_{L_{\alpha_o}}\right)_{exp} + \left(C_{L_{\alpha_F}}\right)_{theory}\right]$$

$$C_{m_{\alpha_I}} = \left(C_{m_{\alpha_{WF}}}\right)_{exp} - \left[\left(C_{m_{\alpha_o}}\right)_{exp} + \left(C_{m_{\alpha_F}}\right)_{theory}\right]$$

Experimental values were used in calculating the contributions to lift and pitching moment of the external wing for the following reasons: The contribution to lift of the external wing is large when compared with the contribution of the wing carry-through section; consequently, a small error introduced in the wing contribution to lift results in a much larger error when expressed in terms of the contribution of the carry-through section as can be seen from the formula. It was therefore believed that, by use of experimental values of wing lift and aerodynamic-center location in the preceding formulas, a more accurate contribution of the carry-through-section lift and, hence, to moment could be obtained. Table II presents the experimental value of $C_{L_{\alpha_{WF}}}$ and $C_{m_{\alpha_{WF}}}$ which were used in calculating the values of $C_{L_{\alpha_I}}$ and $C_{m_{\alpha_I}}$.

A plot of values of $C_{L'_{\alpha_I}}$ (based on carry-through area) with sweep angle of the quarter-chord line $\Lambda_{c/4}$ is shown in figure 6. This lift-curve slope of the carry-through section appears to be fairly consistent about a value of 0.055 per degree for the configurations checked. A somewhat better correlation with experiment was obtained, however, by another method of analysis. A plot of $C_{L'_{\alpha_I}}/c_{l_{\alpha_i}}$ (the lift-curve slope of the carry-through section in terms of the intersection-chord lift-curve slope) against Y/c_i (fig. 4(a)) indicates that the loading of the carry-through section varies with the loading of the adjacent wing and also varies inversely with effective aspect ratio of the carry-through section. A check point obtained from actual integration of the experimental loading of the carry-through section presented in figure 5 is shown in figures 4 and 6.

An examination of figure 4(a) reveals that, as the effective aspect ratio of the carry-through section approaches zero, the value of the ratio $C_{L'_{\alpha_I}}/c_{l_{\alpha_i}}$ exceeds the value of unity. This fact may be explained by an examination of figure 5. The loading of the carry-through section is found to include part of the adjacent-fuselage loading fore and aft of the carry-through section and, since this loading is based on the carry-through area, the wing-induced fuselage loading may possibly exceed the adjacent intersection-chord loading. When the effective aspect ratio of the carry-through section approaches zero, however, the value of the ratio $C_{L'_{\alpha_I}}/c_{l_{\alpha_i}}$ must approach unity. In the absence of experimental data in the region below $\frac{Y}{c_i} = 0.325$ (fig. 4(a)) no attempt has been made to fair the curve to zero effective aspect ratio.

The chordwise aerodynamic-center location of the carry-through section is shown in figure 4(b) as a plot of $\left(\frac{x_i}{c_i}\right)_{LE} - \left(\frac{x_I}{c_i}\right)_{ac}$ (measured from the leading edge of the intersection chord) against $\Lambda_{c/4}$. Shown also in figure 4(b) is the chordwise variation with sweep of the aerodynamic-center location for the center chord as given by the flat-plate first-approximation theory (reference 8). The experimental values show approximately the same variation with sweep as the flat-plate theory except at high-sweep angles. The experimental values also tended to show some effects of the Reynolds number. For a constant sweep angle a higher Reynolds number resulted in a more rearward location of the computed aerodynamic center. Because of the lack of additional experimental points, only one curve has been faired in figure 4(b). The check point obtained from actual integration of the loading of the carry-through section (fig. 5) is also shown in figure 4(b) and shows good agreement.

The configurations used in obtaining the loading and aerodynamic center of the carry-through section shown in figures 4 and 6 and the check configuration are listed as the first 10 configurations in tables I and II. For these 10 configurations sufficient experimental data were presented to obtain the loading on the carry-through section. The static longitudinal stability of the 23 wing-fuselage configurations was calculated by using the curves faired through the experimental data in figure 4 and by the present method.

CORRELATION OF RESULTS

The method has been used to determine the static longitudinal stability of the 23 wing-fuselage configurations listed in table I and the results are presented and compared with the experimental results in table II and figures 7 to 9. A comparison between the experimental and calculated values of lift-curve slopes is presented in figure 7. The calculated values show some disagreement with experiment, however, the disagreement was found to result mostly from low values of $C_{L_{\alpha_W}}$ (theoretical) for wings with approximately 45° sweep angle.

A comparison between the experimental and the calculated values of pitching-moment-curve slopes for the configurations is presented in figure 8. The results of the calculations show reasonable agreement with the experimental values. The disagreement which exists, however, can be traced primarily to the disagreement in lift-curve slopes and to the limitations in estimating the aerodynamic-center location for some of the lift contributing parts. Calculation of the aerodynamic-center location of the wing carry-through section shows that there are probable Reynolds number effects which have not been considered in the method.

A comparison between the experimental and calculated neutral points for the various configurations is presented in figure 9. The agreement, which is generally better than ±0.04, is considered to be good, especially for such a large variety of wing plan forms. The accuracy with which the aerodynamic center and the lift-curve slope of the wing can be determined to a large extent determines the accuracy of the neutral-point location for a wing-fuselage configuration.

CONCLUDING REMARKS

A method is given for calculating the stick-fixed longitudinal stability of a wing-fuselage configuration with unswept or swept wings at subcritical Mach numbers. The stability parameters estimated by the method show reasonable agreement with the experimental values for the 23 configurations used in the comparison. Calculated values of lift-curve slope show some disagreement with experiment at sweep angles close to 45°. This disagreement is found to result mostly from low theoretical values of wing lift-curve slope. The effect of the low values of wing lift-curve slope is also apparent in the calculated values of the slope of the pitching-moment curve. There are noticeable Reynolds number effects on the aerodynamic-center location for the wing and wing carry-through section. As no definite trend of these effects was established, the effects are not considered in the method. To a large extent the accuracy with which the wing stability parameters can be obtained determines the accuracy to which the configuration stability parameters can be calculated.

For the wing carry-through section no theory was available for predicting the loading; therefore, the loading was obtained from curves based on experiment. The experimental lift-curve slope of the wing carry-through section calculated in terms of the carry-through area appears to be consistent about a value of 0.055 per degree. A better correlation with experiment, however, indicates that the carry-through-section loading varies with the loading on the adjacent wing section and also varies inversely with the effective aspect ratio of the carry-through section.

The method has been used to calculate the neutral points of 23 configurations. The agreement between experimental and calculated values has generally been better than ±0.04 and is considered to be good especially for such a large variety of wing plan forms.

Langley Aeronautical Laboratory
National Advisory Committee for Aeronautics
Langley Field, Va.

APPENDIX

SAMPLE CALCULATIONS

The contributions to lift-curve and pitching-moment-curve slopes and the aerodynamic-center location were calculated for wing-fuselage configuration 4 (see tables I and II) by the method presented in this paper. These calculations are presented as an aid to further understanding the method. The steps are numbered to correspond with the steps presented in the section "Calculation of Stability." Two views of the model are shown in figure 10 which was obtained from reference 9. Some total wing parameters used in the example are as follows:

$A = 3.5$

$\bar{Y} = 3.6$ feet

$b = 27$ feet

$y_{MAC} = 5.4$ feet

$\bar{c} = 8.64$ feet

$\lambda = 0.25$

$c_{av} = 7.72$ feet

$\Lambda_{c/4} = 60.8^\circ$

$S_W = 208.3$ square feet

External Wing

Calculation of $C_{L_{\alpha_O}}$.- Steps used in calculating $C_{L_{\alpha_O}}$ are:

(1) From reference 3, figure 4, $C_{L_{\alpha_W}} = 0.0412$.

(2) $C_{L_{\alpha_W}} S_W = (0.0412)(208.3) = 8.60$ square feet

(3) From reference 3, figure 3:

For $\eta = 0$

$$\frac{c_{l_a} c}{C_L c_{av}} = 1.13 = \frac{c_{l_\alpha} c}{C_{L_{\alpha_W}} c_{av}}$$

For $\eta = 0.13$

$$\frac{c_{l_a}c}{C_L c_{av}} = 1.15 = \frac{c_{l_\alpha}c}{C_{L_{\alpha_W}} c_{av}}$$

(4) $$c_{l_\alpha}c = \frac{c_{l_\alpha}c}{C_{L_{\alpha_W}} c_{av}} C_{L_{\alpha_W}} c_{av}$$

For $\eta = 0$

$$c_{l_\alpha}c = (1.13)(0.0412)(7.72) = 0.359 \text{ feet}$$

For $\eta = 0.13$

$$c_{l_\alpha}c = (1.15)(0.0412)(7.72) = 0.365 \text{ feet}$$

(5) See figure 11 for plot of local wing loading $c_{l_\alpha}c$ against wing spanwise station.

(6) $$C_{L_{\alpha_\sigma}} S_\sigma = \left(c_{l_\alpha}c\right)_{av} Y$$

$$= \frac{0.359 + 0.365}{2} 3.6 = 1.302 \text{ square feet}$$

(7) $$C_{L'_{\alpha_o}} S_o = C_{L_{\alpha_W}} S_W - C_{L_{\alpha_\sigma}} S_\sigma$$

$$= 8.60 - 1.302 = 7.298 \text{ square feet}$$

(8) $$C_{L_{\alpha_o}} = \frac{C_{L'_{\alpha_o}} S_o}{S_W}$$

$$= \frac{7.298}{208.3} = 0.0349$$

Calculation of $C_{m_{\alpha_o}}$.- Steps for calculating $C_{m_{\alpha_o}}$ are:

(1) From reference 3, figure 5(b), $\eta_{cp} = 0.449$.

$$y_{W_{cp}} = \eta_{cp} \frac{b}{2} = 0.449(13.5) = 6.06 \text{ feet}$$

[redacted]

(2) $$y_{\sigma_{cp}} = \frac{1}{2}\frac{Y}{2}$$

$$= \frac{1}{2}(1.8) = 0.9 \text{ foot}$$

(3) $$y_{o_{cp}} = \frac{C_{L_{\alpha_W}} S_W y_{W_{cp}} - C_{L_{\alpha_\sigma}} S_\sigma y_{\sigma_{cp}}}{C_{L_{\alpha_W}} S_W - C_{L_{\alpha_\sigma}} S_\sigma}$$

$$= \frac{(8.6)(6.06) - (1.302)(0.9)}{8.6 - 1.302} = 6.99 \text{ feet}$$

(4) $$C_{m_{\alpha_o}} = \frac{y_{MAC} - y_{o_{cp}}}{\bar{c}} \tan \Lambda_{c/4} C_{L_{\alpha_o}}$$

$$= \frac{5.4 - 6.99}{8.64}(1.789)(0.0349) = -0.0115$$

Fuselage

Calculation of $C_{L_{\alpha_F}}$ and $C_{m_{\alpha_F}}$.- Calculation of the fuselage sectional lift is shown in table III and plotted in figure 12. The fuselage contribution to lift and pitching moment obtained from an integration of the fuselage sectional lift in figure 12 is found to be

$$C_{L_{\alpha_F}} = 0.00177$$

$$C_{m_{\alpha_F}} = 0.00366$$

Wing Carry-Through Section

Some wing carry-through-section parameters are as follows:

$$\frac{Y}{c_i} = 0.32$$

$$S_I = Yc_i = (3.6)(11.25) = 40.5 \text{ square feet}$$

$$x_i = 9.33$$

$$c_{l_{\alpha_i}} = 0.0325$$

Calculation of $C_{L_{\alpha_I}}$.- Steps for obtaining $C_{L_{\alpha_I}}$ follow:

(1) From figure 4(a), $\dfrac{C_{L'_{\alpha_I}}}{c_{l_{\alpha_i}}} = 1.42$

(2)
$$C_{L_{\alpha_I}} = \frac{C_{L'_{\alpha_I}}}{c_{l_{\alpha_i}}} c_{l_{\alpha_i}} \frac{S_I}{S_W}$$

$$= 1.42(0.0325)\frac{40.5}{208.3} = 0.00896$$

Calculation of $C_{m_{\alpha_I}}$.- Steps for calculating $C_{m_{\alpha_I}}$ are:

(1) From figure 4(b), $\left(\dfrac{x_i}{c_i}\right)_{LE} - \left(\dfrac{x_I}{c_i}\right)_{ac} = 0.68$

(2)
$$\left(\frac{x_I}{c_i}\right)_{ac} = \left(\frac{x_i}{c_i}\right)_{LE} - \left[\left(\frac{x_i}{c_i}\right)_{LE} - \left(\frac{x_I}{c_i}\right)_{ac}\right]$$

$$= \frac{9.33}{11.25} - 0.68 = 0.15$$

(3)
$$C_{m_{\alpha_I}} = \left(\frac{x_I}{c_i}\right)_{ac} \frac{c_i}{\bar{c}} C_{L_{\alpha_I}}$$

$$= (0.15)\frac{11.25}{8.64}(0.00896) = 0.00175$$

Complete Configuration

Calculation of $C_{L_{\alpha_{WF}}}$.- Values of lift-curve slopes for the complete configuration are:

Estimated value by present method

$$C_{L_{\alpha_{WF}}} = C_{L_{\alpha_o}} + C_{L_{\alpha_F}} + C_{L_{\alpha_I}}$$

$$= 0.0349 + 0.00177 + 0.00896 = 0.0456$$

Experimental value (table II)

$$C_{L_{\alpha_{WF}}} = 0.047$$

Calculation of $C_{m_{\alpha_{WF}}}$.- The pitching-moment-curve slopes for the complete configuration are:

Estimated value by present method

$$C_{m_{\alpha_{WF}}} = C_{m_{\alpha_O}} + C_{m_{\alpha_F}} + C_{m_{\alpha_I}}$$

$$= -0.0115 + 0.00366 + 0.00175 = -0.00609$$

Experimental value (table II)

$$C_{m_{\alpha_{WF}}} = -0.0061$$

Calculation of neutral-point location.- The neutral-point location is calculated to be:

Estimated value by present method

$$\frac{C_{m_{\alpha_{WF}}}}{C_{L_{\alpha_{WF}}}} = \frac{x_{WF}}{\bar{c}}$$

$$\frac{-0.00609}{0.0456} = -0.134$$

Experimental value (table II)

$$\frac{C_{m_{\alpha_{WF}}}}{C_{L_{\alpha_{WF}}}} = \frac{x_{WF}}{\bar{c}}$$

$$\frac{-0.061}{0.047} = -0.13$$

REFERENCES

1. White, Maurice D.: Estimation of Stick-Fixed Neutral Points of Airplanes. NACA CB L5C01, 1945.

2. Multhopp, H.: Aerodynamics of the Fuselage. NACA TM 1036, 1942.

3. DeYoung, John, and Harper, Charles W.: Theoretical Symmetric Span Loading at Subsonic Speeds for Wings Having Arbitrary Plan Form. NACA Rep. 921, 1948.

4. Hess, Robert V., and Gardner, Clifford S.: Study by the Prandtl-Glauert Method of Compressibility Effects and Critical Mach Number for Ellipsoids of Various Aspect Ratios and Thickness Ratios. NACA TN 1792, 1949.

5. Schlichting, H.: Calculation of the Influence of a Body on the Position of the Aerodynamic Centre of Aircraft with Sweptback Wings. TN No. Aero 1879, British R.A.E., March 1947.

6. Toll, Thomas A., and Queijo, M. J.: Approximate Relations and Charts for Low-Speed Stability Derivatives of Swept Wings. NACA TN 1581, 1948.

7. Schlichting, H.: Aerodynamics of the Mutual Influence of Aircraft Parts (Interference). Library Translation No. 275, British R.A.E., Oct. 1948.

8. Kücheman, D., and Weber, J.: On the Chordwise Lift Distribution at the Centre of Swept Wings. Aeronautical Quarterly, vol. II, pt. II, Aug. 1950, pp. 146-155.

9. McCormack, Gerald M., and Walling, Walter C.: Aerodynamic Study of a Wing-Fuselage Combination Employing a Wing Swept Back 63°. - Investigation of a Large-Scale Model at Low Speeed. NACA RM A8D02, 1949.

10. Spearman, M. Leroy, and Comisarow, Paul: An Investigation of the Low-Speed Static Stability Characteristics of Complete Models Having Sweptback and Sweptforward Wings. NACA RM L8H31, 1948.

11. Spooner, Stanley H., and Mollenberg, Ernst F.: Positioning Investigation of Single Slotted Flaps on a 47.7° Sweptback Wing at Reynolds Numbers of 4.0×10^6 and 6.0×10^6. NACA RM L50H29, 1950.

12. Schuldenfrei, Marvin, Comisarow, Paul, and Goodson, Kenneth W.: Stability and Control Characteristics of a Complete Airplane Model Having a Wing with Quarter-Chord Line Swept Back 40°, Aspect Ratio 2.50, and Taper Ratio 0.42. NACA TN 2482, 1951. (Formerly NACA RM L7B25.)

13. Foster, Gerald V., and Fitzpatrick, James E.: Longitudinal-Stability Investigation of High-Lift and Stall-Control Devices on a 52° Sweptback Wing with and without Fuselage and Horizontal Tail at a Reynolds Number of 6.8×10^6. NACA RM L8I08, 1948.

14. Bird, John D., Lichtenstein, Jacob H., and Jaquet, Byron M.: Investigation of the Influence of Fuselage and Tail Surfaces on Low-Speed Static Stability and Rolling Characteristics of a Swept-Wing Model. NACA RM L7H15, 1947.

15. Conner, D. William, and Neely, Robert H.: Effects of a Fuselage and Various High-Lift and Stall-Control Flaps on Aerodynamic Characteristics in Pitch of an NACA 64-Series 40° Swept-Back Wing. NACA RM L6L27, 1947.

16. Spooner, Stanley H., and Martina, Albert P.: Longitudinal Stability Characteristics of a 42° Sweptback Wing and Tail Combination at a Reynolds Number of 6.8×10^6. NACA RM L8E12, 1948.

17. Salmi, Reino J., Conner, D. William, and Graham, Robert R.: Effects of a Fuselage on the Aerodynamic Characteristics of a 42° Sweptback Wing at Reynolds Numbers to 8,000,000. NACA RM L7E13, 1947.

18. Möller, E.: Systematische Sechskomponentenmessungen an Flügel/Rumpfanordnungen mit Pfeilflügeln konstanter Tiefe. Forschungsbericht Nr. 1318/4, Deutsche Luftfahrtforschung (Braunschweig), 1943.

TABLE I

DIMENSIONS AND INFORMATION ON CONFIGURATIONS

Configuration	Configuration number	Symbol	NACA airfoil	$\Lambda_{c/4}$ (deg)	λ	A	b (ft)	$\bar{c}$ (ft)	Y (ft)	c_i (ft)	S_W (sq ft)	Reynolds number	Reference
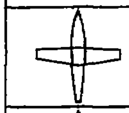	1	○	65-110	0	0.50	6	7	1.202	1.14	1.42	8.125	1.94×10^6	10
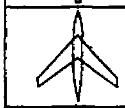	2	□	64-210	45	.383	5.1	12.46	2.6	1.4	3.28	30.35	6.0	11
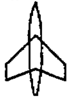	3	◇	65-110	40	.42	2.5	5.83	2.47	1.147	2.91	13.64	2.87	12
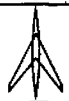	4	△	[a]64A006	60.8	.25	3.5	27	8.639	3.6	11.25	208.3	8.00	9
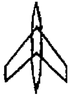	5	▽	64_1-112	50	.625	2.88	9.41	3.33	1.4	3.8	30.75	6.80	13
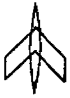	6	▷	0012	45	1	2.63	3.04	1.18	0.5	1.18	3.50	1.40	14
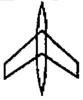	7	◁	64_1-112	40	.625	4.01	11.35	2.89	1.4	3.34	32.24	3.04	15
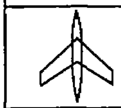	8	◸	64_1-112	40	.625	4.01	11.35	2.89	1.4	3.34	32.24	6.84	15 and 16
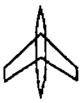	9	◹	64_1-112	40	.625	4.01	11.35	2.89	1.4	3.34	32.24	8.09	15 and 17
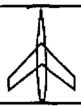	10	◺	[a]65A006	45	.6	4	2	0.51	0.267	0.59	1.00	1.73	Unpublished
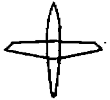	11	◿	65-110	0	.445	6.8	7.68	1.181	1.14	1.42	8.67	1.27	10
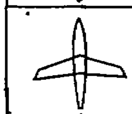	12	D	65-110	15	.461	6.4	7.29	1.20	1.10	1.43	8.40	1.292	10

[a]Airfoil parallel to plane of symmetry (airfoils not-footnoted perpendicular to 0.25-chord line).

TABLE I - Concluded

DIMENSIONS AND INFORMATION ON CONFIGURATIONS - Concluded

Configuration	Configuration number	Symbol	NACA airfoil	$\Lambda_{c/4}$ (deg)	λ	A	b (ft)	$\bar{c}$ (ft)	$\bar{Y}$ (ft)	c_i (ft)	S_W (sq ft)	Reynolds number	Reference
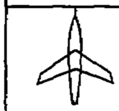	13	□	65-110	30	0.46	5.24	6.50	1.278	1.10	1.53	8.06	1.373×10^6	10
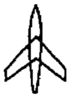	14	□	65-110	45	.465	3.69	5.36	1.542	1.10	1.79	7.80	1.657	10
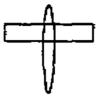	15	□	23012	0	1	5.18	2.53	.492	.328	.492	1.231	-----	18
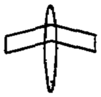	16	□	23012	15	1	5.18	2.53	.492	.328	.492	1.231	-----	18
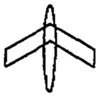	17	□	23012	30	1	5.18	2.53	.492	.328	.492	1.231	-----	18
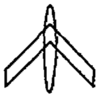	18	□	23012	45	1	5.18	2.53	.492	.328	.492	1.231	-----	18
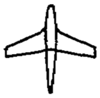	19	□	$^{c}64_{(10)}$-010.3 64-008	20	.463	5.74	7.72	1.396	.917	1.85	10.39	1.40	Unpublished
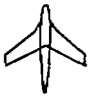	20	▽	$^{c}64_{(10)}$-010.3 64-008	35	.459	4.53	6.90	1.579	.917	2.01	10.5	1.59	Unpublished
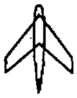	21	△	$^{c}64_{(10)}$-010.3 64-008	50	.454	2.95	5.67	1.985	.917	2.40	10.9	2.00	Unpublished
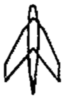	22	◁	$^{c}64_{(10)}$-010.3 64-008	60	.445	1.90	4.66	2.535	.917	2.77	11.47	2.56	Unpublished
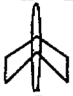	23	▷	^{b,d}R-4 40-1$_7$10-1$_1$0	37.5	1.63	3.07	31.3	10.59	4.6	8.6	320	9.3	Unpublished

[b] Airfoil perpendicular to 0.50-chord line, (airfoils not-footnoted perpendicular to 0.25-chord line).

[c] Root chord; tip chord.

[d] Republic airfoil section.

[redacted]

[redacted]

[redacted]

TABLE II

CALCULATED AND EXPERIMENTAL VALUES FOR CONFIGURATIONS

Configuration number	Symbol	Experimental $C_{L_{\alpha_W}}$	Experimental $\frac{x_W}{c}$	Calculated $C_{L_{\alpha_0}}$	Calculated $C_{m_{\alpha_0}}$	Calculated $C_{L_{\alpha_F}}$	Calculated $C_{m_{\alpha_F}}$	Calculated $C_{L'}{}_{\alpha_I}$	Calculated $\left(\frac{x_i}{c_i}\right)_{LE} - \left(\frac{x_I}{c_i}\right)_{ac}$	Experimental $C_{L_{\alpha_{WF}}}$	Experimental $C_{m_{\alpha_{WF}}}$	Calculated $C_{L_{\alpha_{WF}}}$	Calculated $C_{m_{\alpha_{WF}}}$	Experimental $\frac{x_{WF}}{c}$	Theoretical $\frac{x_{WF}}{c}$
1	○	0.074	0.282	0.0597	0	0.0096	0.0132	0.0547	0.28	0.079	0.0144	0.0805	0.0125	0.182	0.156
2	□	.062	-.0735	.0501	-.0094	.0022	.0050	.058	.52	.0645	-.0026	.0598	-.0010	-.04	-.018
3	◇	.046	.007	.0358	-.0040	.0034	.0045	.0473	.40	.05	.0016	.0516	.0003	.031	.0054
4	△	.042	-.13	.0349	-.0105	.0018	.0037	.0485	.77	.047	-.0061	.0456	-.0061	-.13	-.134
5	▽	.046	-.0025	.0366	-.0041	.0021	.0036	.0525	.54	.05	0	.0474	.0012	0	.0247
6	▷	.046	.054	.0376	-.0005	.0022	.0026	.0545	.54	.049	.0032	.0448	.0019	.065	.042
7	◁	.060	.008	.0466	-.0046	.0022	.0043	.0745	.42	.062	.0029	.0567	.0023	.047	.041
8	◸	.060	-.003	.0466	-.0046	.0022	.0043	.0634	.44	.062	.0016	.0567	.0023	.027	.041
9	◹	.061	.0145	.0466	-.0046	.0022	.0043	.0675	.50	.064	.0019	.0567	.0023	.03	.041
10	◺	-----	------	.0448	-.0057	.0027	.0051	.0431	.52	.062	.0012	.0550	.0020	.02	.037
11	◿	-----	------	.0646	0	.009	.0126	------	----	.0876	.0158	.0845	.0119	.18	.141
12	▽	-----	------	.0616	-.0037	.0078	.0140	------	----	.0834	.0110	.0792	.0113	.132	.143
13	◁	-----	------	.0529	-.0068	.0067	.0140	------	----	.0706	.0059	.069	.0091	.083	.132
14	▷	-----	------	.0392	-.0080	.0060	.0119	------	----	.06	.0025	.0547	.0050	.0417	.0905
15	◿	-----	------	.0583	0	.0038	.0037	------	----	.0694	.0035	.0701	.0033	.05	.048
16	⌓	-----	------	.0568	-.0007	.0034	.0046	------	----	.0688	.0050	.0676	.0050	.072	.074
17	◡	-----	------	.053	-.0020	.0033	.0054	------	----	.0616	.0071	.0626	.0059	.115	.095
18	D	-----	------	.0461	-.0046	.0030	.0066	------	----	.0523	.0078	.0541	.0056	.15	.1027
19	ᗡ	-----	------	.0628	-.0033	.0030	.0048	------	----	.0796	.0035	.0786	[a].0054	.0434	.069
20	⬠	-----	------	.0524	-.0056	.0025	.0038	------	----	.0675	-.0012	.0649	[a].0022	-.0176	.0333
21	⬡	-----	------	.0353	-.0068	.0022	.0027	------	----	.049	-.0036	.0491	[a]-.0022	-.074	-.0438
22	⬡	-----	------	.0262	-.0048	.0021	.0018	------	----	.0386	-.005	.0378	[a]-.0036	-.13	-.096
23	○	-----	------	.038	.0005	.0029	.0042	------	----	.0544	.0086	.0461	.0062	.159	.135

[a] Contains pitching-moment contribution due to fuselage nose duct.

TABLE III

CALCULATION OF FUSELAGE SECTIONAL LIFT

Fuselage station	x_f (ft)	Y_f (ft)	$\frac{\pi}{2} Y_f^2$ (sq ft)	$x_f - x_{c_i/4}$	$\frac{x_f - x_{c_i/4}}{b}$	κ	$\frac{d\beta}{d\alpha}$	$\frac{\pi}{2} Y_f^2 \frac{d\beta}{d\alpha}$ (sq ft)	$\frac{d\left(\frac{\pi}{2} Y_f^2 \frac{d\beta}{d\alpha}\right)}{dx_f'}$ (ft)
Fore fuselage									
0	25.53	0	0	19.15	0.710	0.020	1.014	0	0
1	24.53	.60	.566	18.15	.672	.021	1.014	.575	.71
2	22.53	1.28	2.580	16.15	.598	.022	1.015	2.620	1.26
3	20.53	1.82	5.210	14.15	.524	.028	1.019	5.310	1.38
4	18.53	2.24	7.900	12.15	.450	.033	1.022	8.080	1.39
5	16.53	2.60	10.600	10.15	.376	.042	1.028	10.900	1.39
6	14.53	2.90	13.210	8.15	.302	.055	1.037	13.700	1.39
7	12.53	3.14	15.500	6.15	.228	.077	1.052	16.320	1.25
8	10.53	3.34	17.550	4.15	.189	.093	1.063	18.680	1.35
9	8.53	3.50	19.300	2.15	.080	.245	1.165	22.500	2.55
Aft fuselage									
10	-3.47	3.50	19.300	-----	-----	-----	0.050	0.965	0.61
11	-5.47	3.34	17.550	-----	-----	-----	.120	2.105	.45
12	-7.47	3.14	15.500	-----	-----	-----	.180	2.790	.26
13	-9.47	2.90	13.210	-----	-----	-----	.240	3.170	.16
14	-11.47	2.60	10.600	-----	-----	-----	.310	3.290	-.04
15	-13.47	2.24	7.900	-----	-----	-----	.370	2.980	-.26
16	-15.47	1.82	5.210	-----	-----	-----	.430	2.240	-.41
17	-17.47	1.28	2.580	-----	-----	-----	.500	1.290	-.51
18	-19.47	.60	.566	-----	-----	-----	.570	.320	-.39
19	-20.47	0	0	-----	-----	-----	.630	0	0

NACA

[redacted]

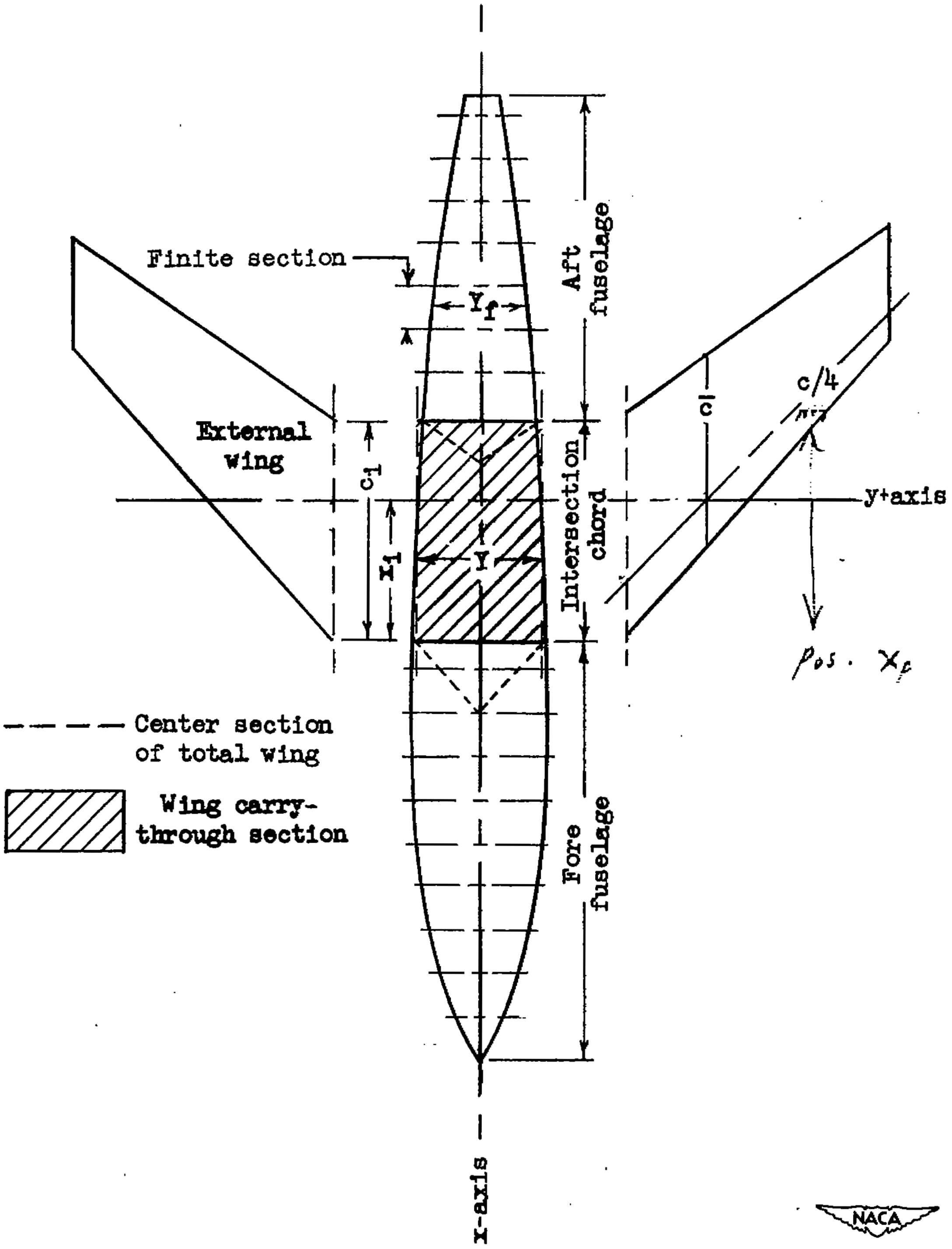
Finite section
Y_f
Aft fuselage
External wing
c_1
x_1
Y
Intersection chord
c
$c/4$
Λ
y-axis
Pos. X_f
Center section of total wing
Wing carry-through section
Fore fuselage
x-axis

Figure 1.- Wing-fuselage configuration illustrating separation of the configuration into the principal parts. Some general notations are included.

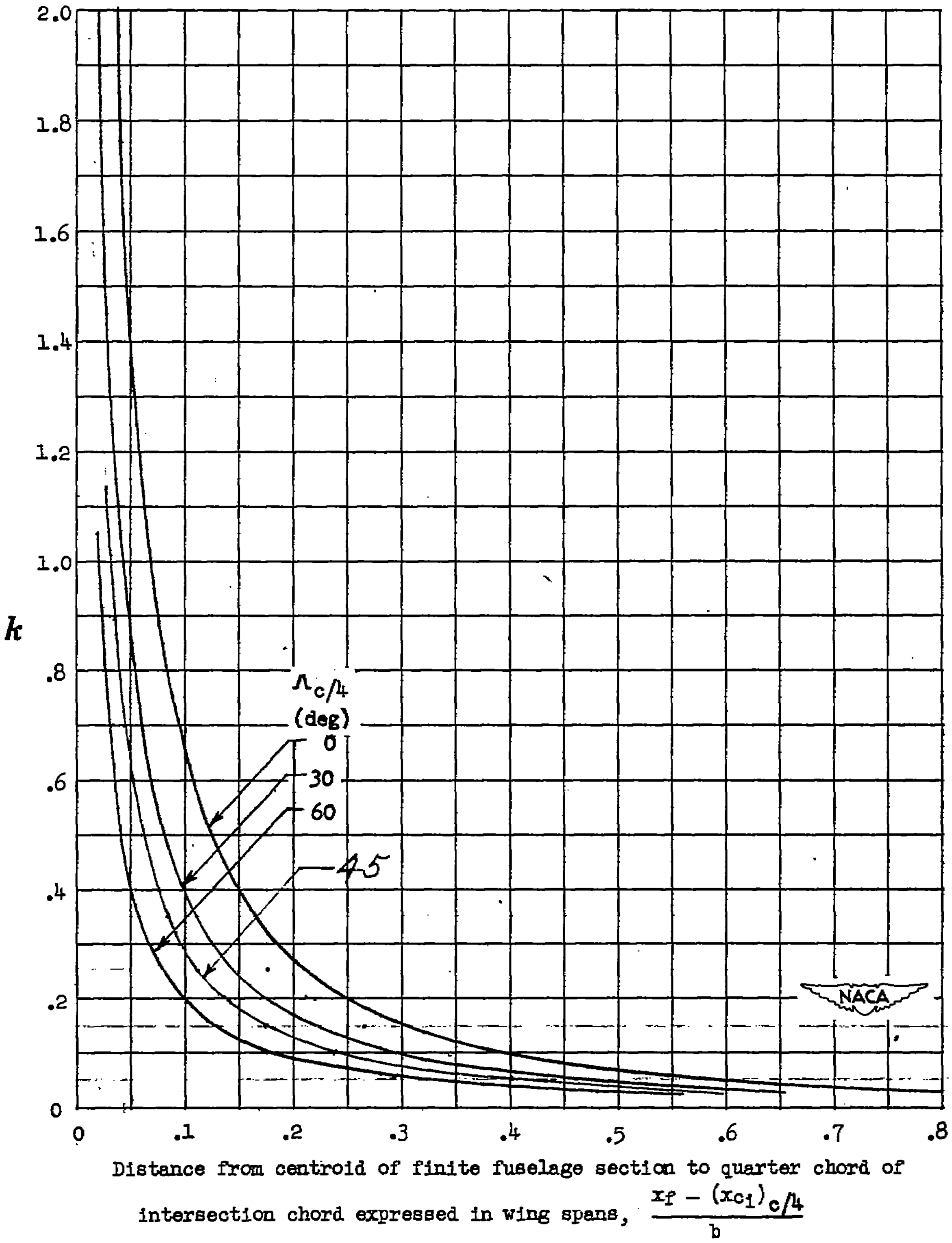

Figure 2.- Variation of values of κ with distance forward from the quarter-chord point of the wing-fuselage intersection chord. (Reference 5.) Values of $d\beta/d\alpha$ may be obtained for wings of various aspect ratios and lift-curve slopes by $\frac{d\beta}{d\alpha} = 1 + \kappa \frac{C_{L_{\alpha_W}}}{A} (57.3)$.

[redacted]

[redacted]

[redacted]

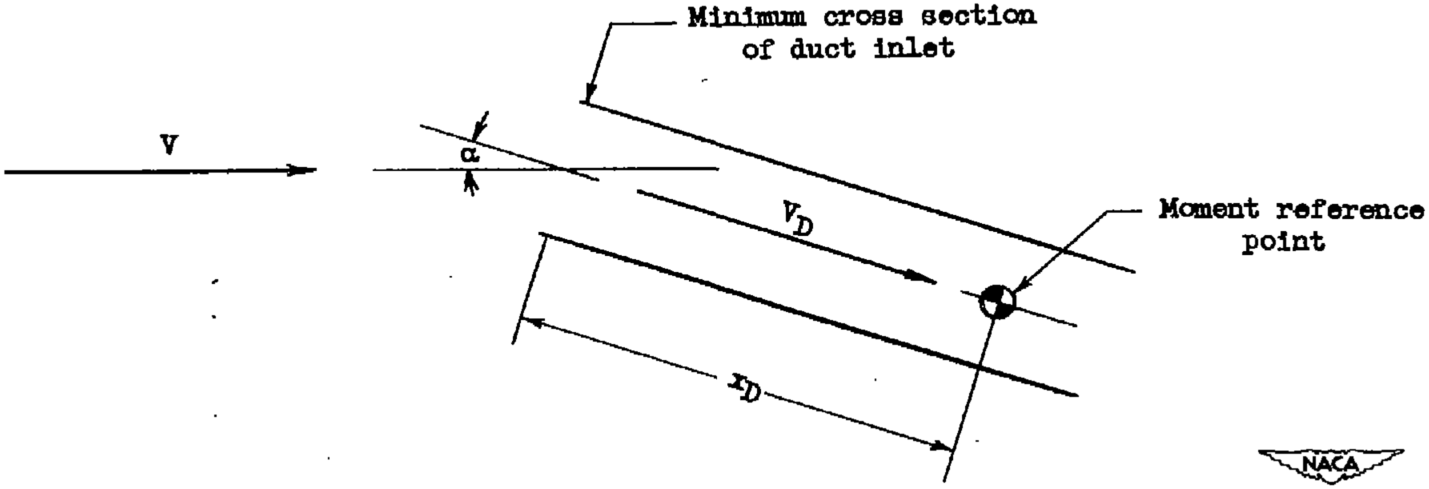
Minimum cross section of duct inlet
V
α
V_D
Moment reference point
x_D

Figure 3.- Diagram showing velocity vectors for calculation of additional pitching-moment contributions contributed by the air mass on the inlet duct. (Unpublished data.)

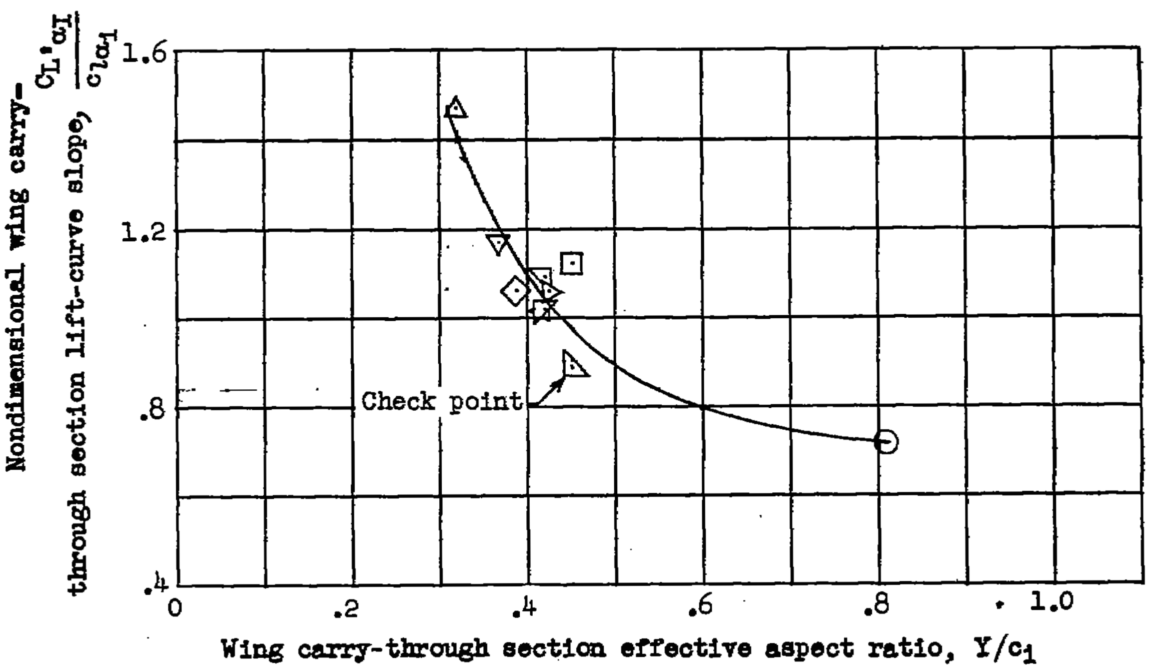

(a) Lift-curve slope.

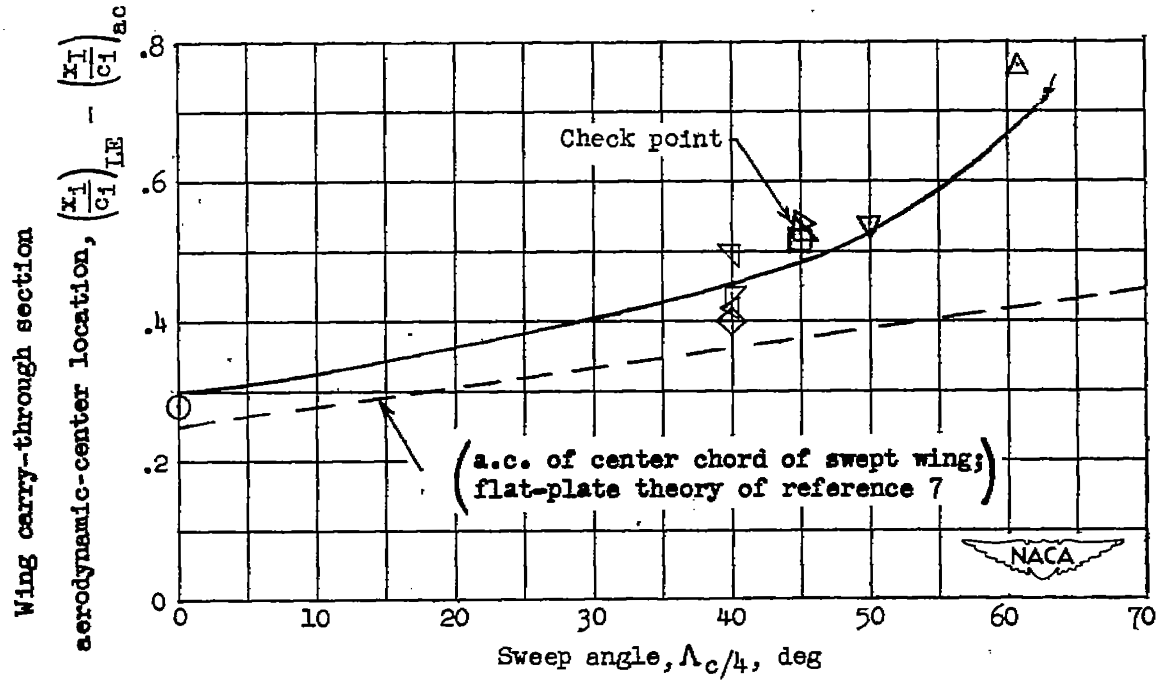

(b) Aerodynamic-center location.

Figure 4.- Lift-curve slope and aerodynamic-center location of wing carry-through section. Symbols refer to configurations listed in tables I and II. Check point refers to actual integration of carry-through loading.

[redacted]

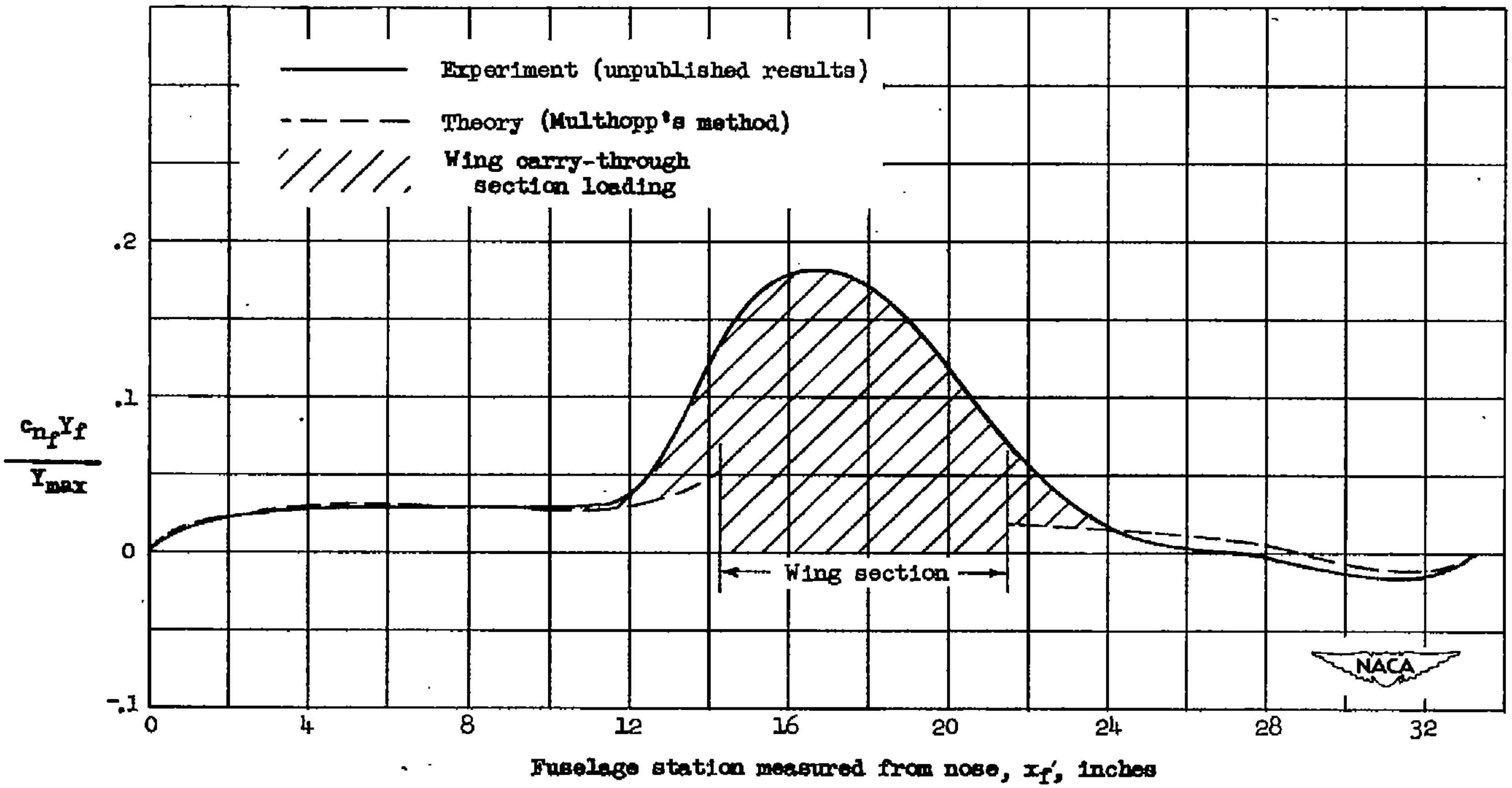

Figure 5.- A comparison between experimental and theoretical fuselage sectional loading. $\alpha = 4^{\circ}$; $M = 0.61$. Configuration 10 of tables I and II.

[redacted]

[redacted]

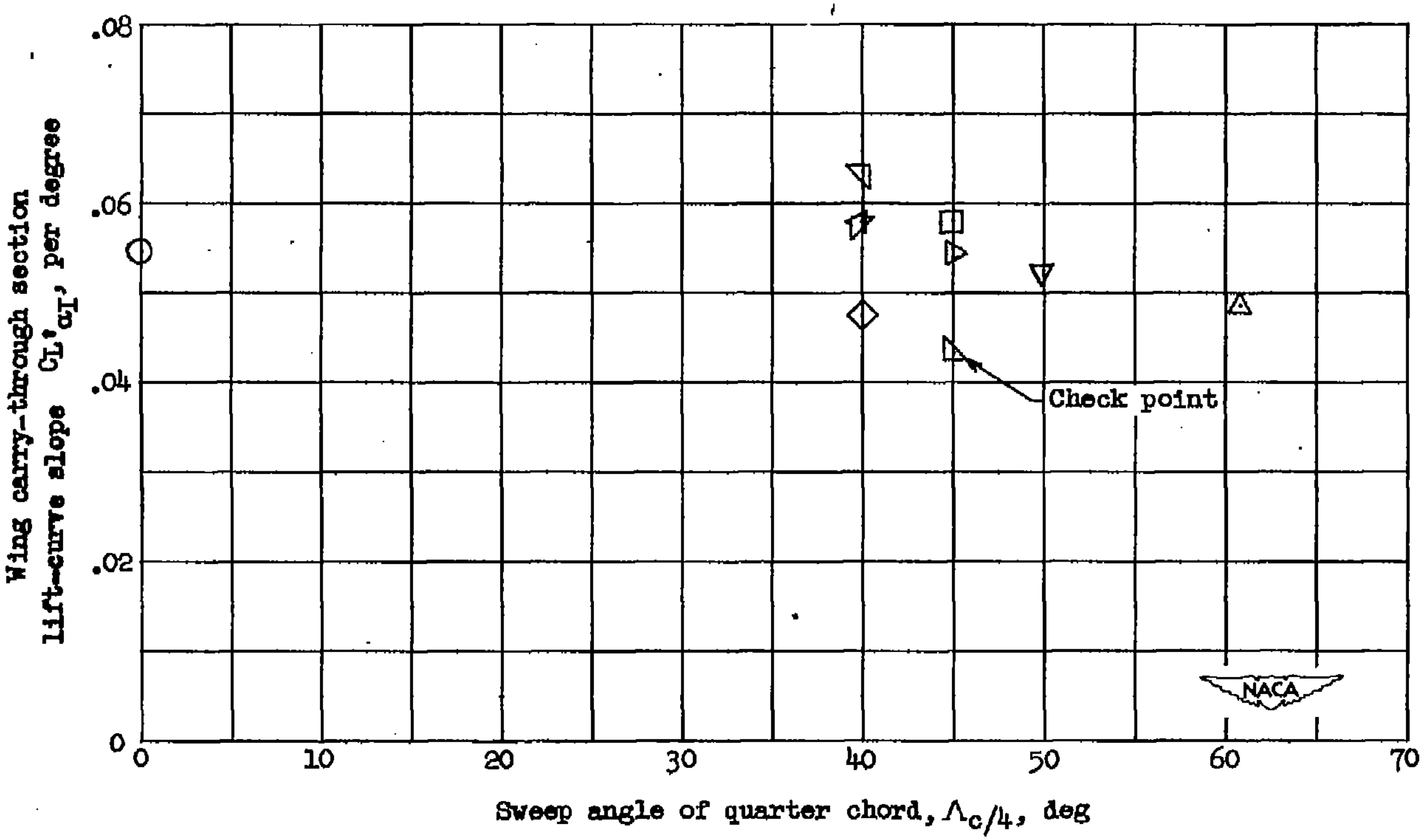

Figure 6.- Wing carry-through section lift-curve slopes (based on wing carry-through section area S_I) for 10 wing-fuselage configurations as obtained by the present method. Symbols refer to configurations of tables I and II. Check point refers to actual integration of carry-through loading.

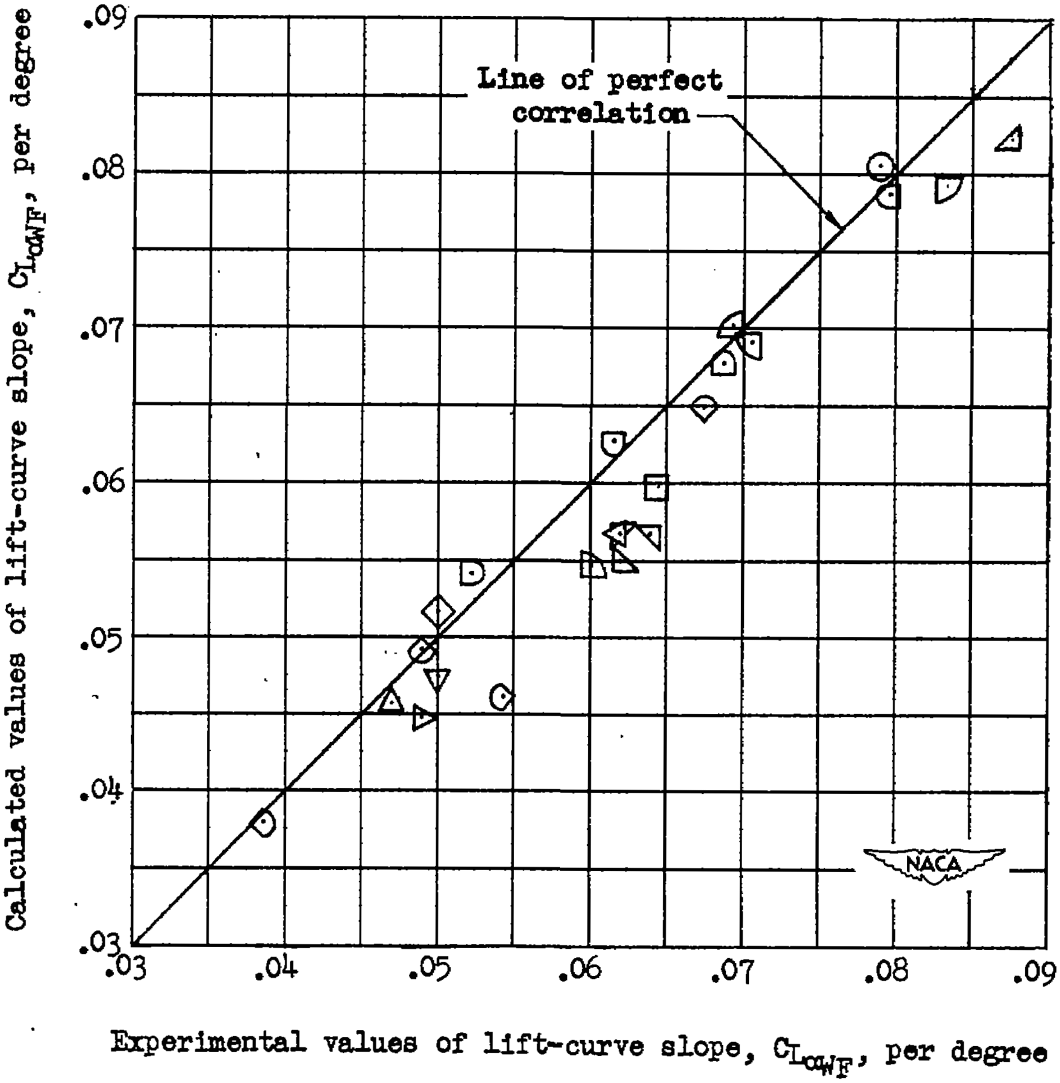

Figure 7.- A comparison between experimental and theoretical values of $C_{L_{\alpha_{WF}}}$ for 23 wing-fuselage configurations. Symbols refer to configurations identified in tables I and II.

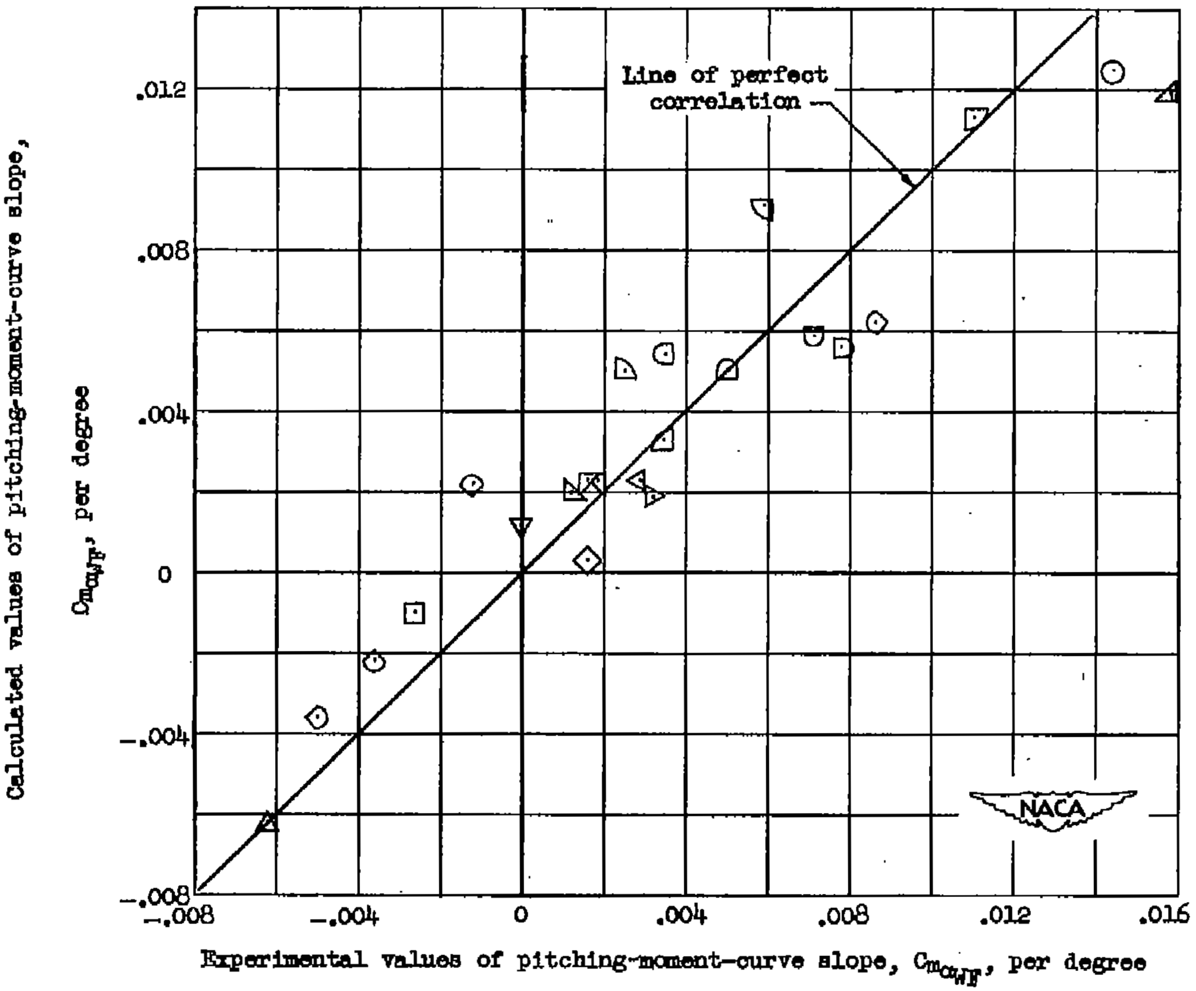

Figure 8.- A comparison between experimental and theoretical values of $C_{m_{\alpha_{WF}}}$ for 23 wing-fuselage configurations. Symbols refer to configurations of tables I and II.

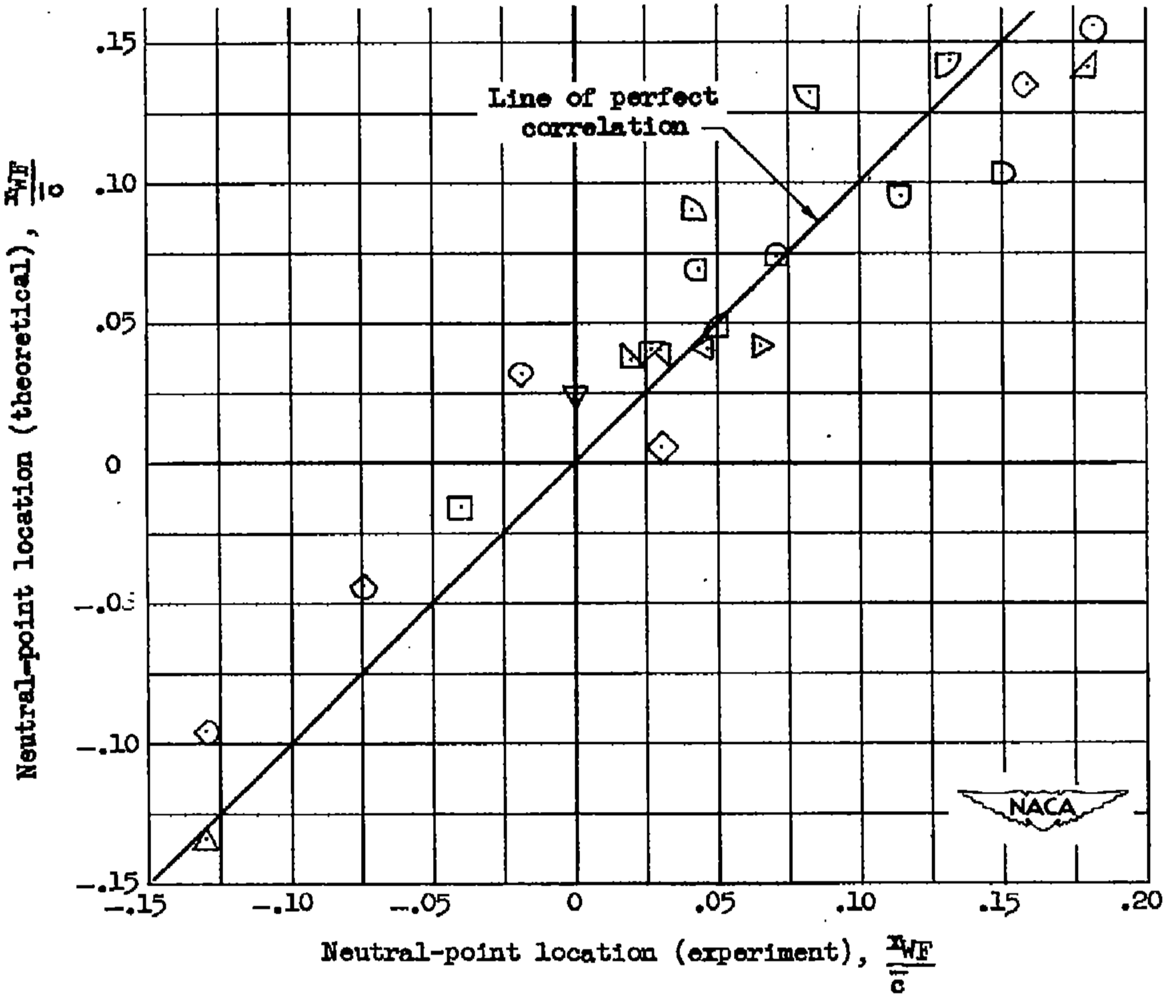

Figure 9.- A comparison between the experimental and calculated stick-fixed neutral points for 23 wing-fuselage configurations. Symbols refer to configurations identified in tables I and II.

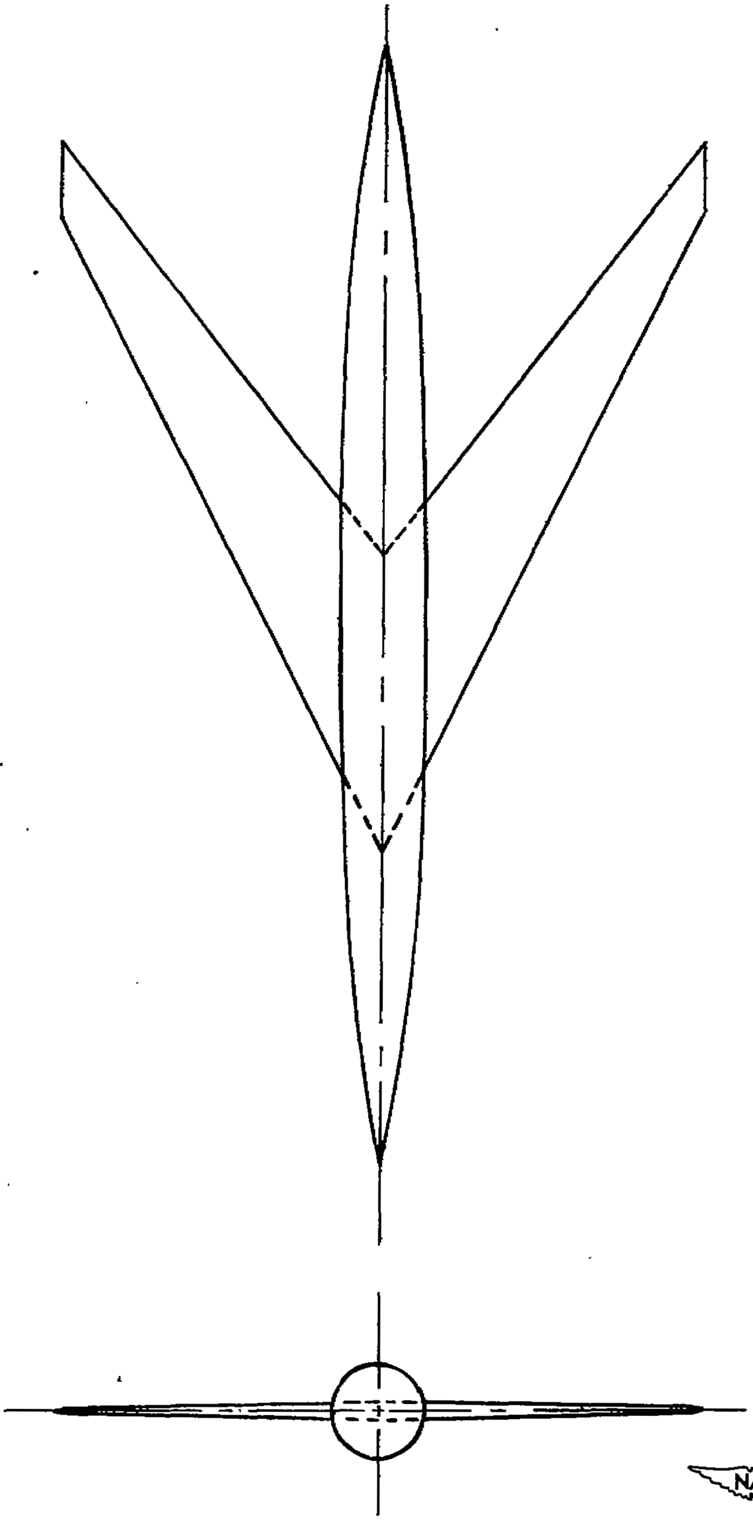

Figure 10.- Two views of sweptback-wing - fuselage configuration. $\Lambda_{c/4} = 60.8^{\circ}$; $A = 3.5$; $\lambda = 0.25$; airfoil section, NACA 64A006. (Reference 9.)

[redacted]

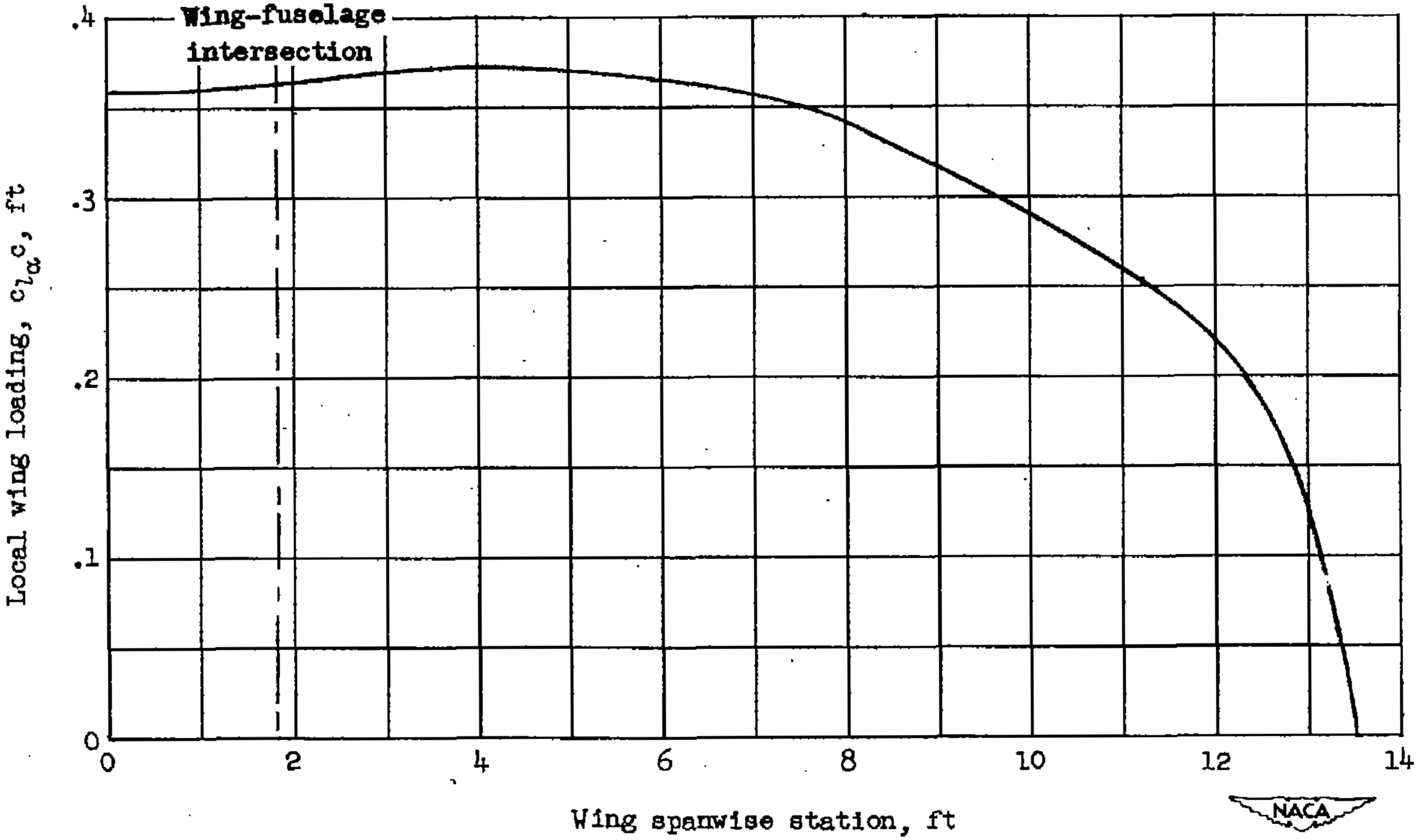

Figure 11.- Spanwise load distribution of wing semispan for configuration 4.

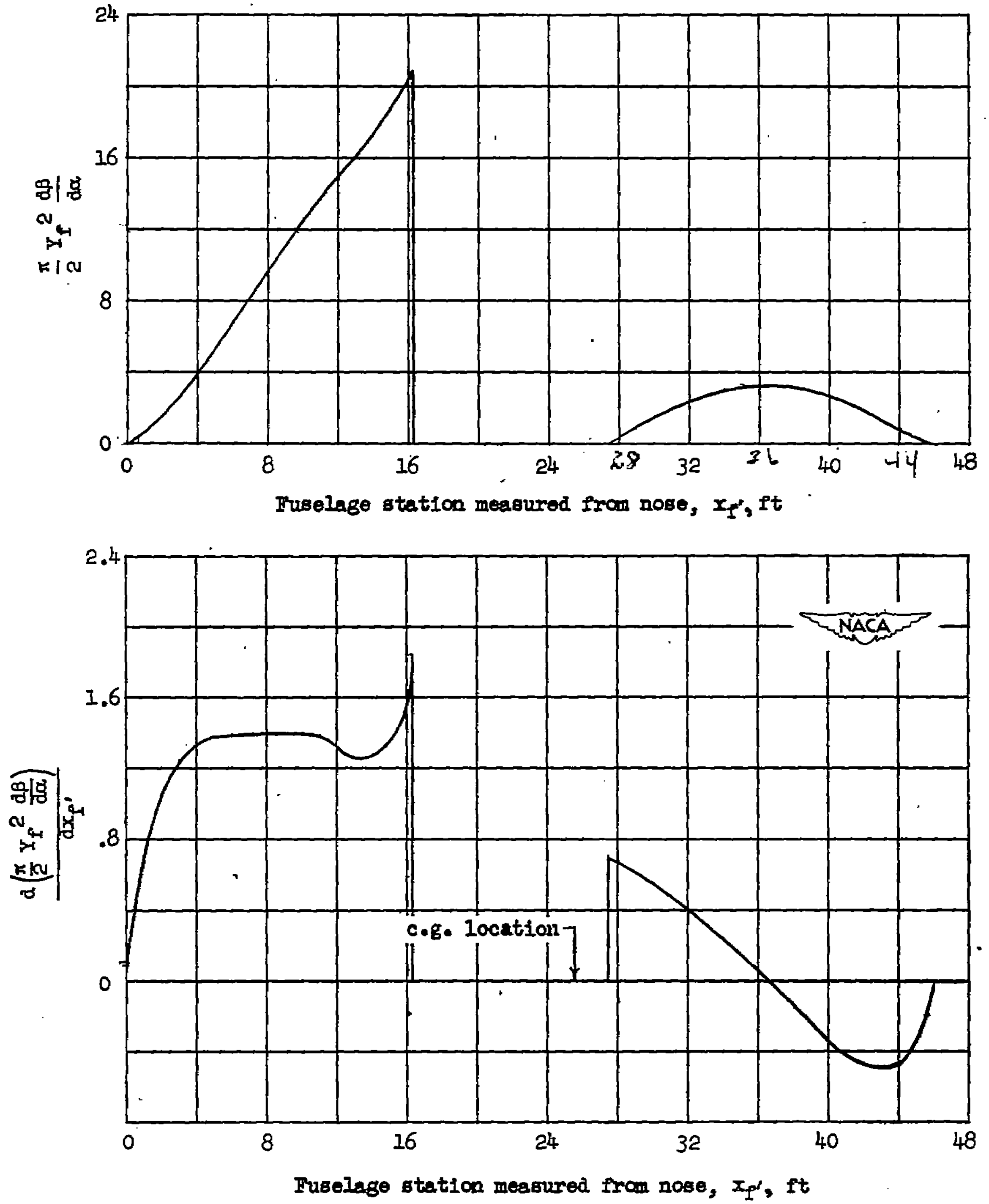

Figure 12.- Calculated fuselage lift distribution.

NACA-Langley - 1-22-52 - 325

SECURITY INFORMATION

NASA Technical Library
3 1176 01436 8923

[redacted]